

Article

Rate Decline Analysis of Vertically Fractured Wells in Shale Gas Reservoirs

Xiaoyang Zhang ^{1,2,3}, Xiaodong Wang ^{1,2,*} , Xiaochun Hou ^{1,2} and Wenli Xu ^{1,3}

¹ School of Energy Resources, China University of Geosciences (Beijing), Beijing 100083, China; z_xyang123@163.com (X.Z.); wysdgilike@163.com (X.H.); xuwl2014@163.com (W.X.)

² Beijing Key Laboratory of Unconventional Natural Gas Geological Evaluation and Development Engineering, Beijing 100083, China

³ Key Laboratory of Strategy Evaluation for Shale Gas, Ministry of Land and Resources, Beijing 100083, China

* Correspondence: wxd_cugb@126.com; Tel.: +86-10-8232-2754

Received: 14 September 2017; Accepted: 6 October 2017; Published: 13 October 2017

Abstract: Based on the porous flow theory, an extension of the pseudo-functions approach for the solution of non-linear partial differential equations considering adsorption-desorption effects was used to investigate the transient flow behavior of fractured wells in shale gas reservoirs. The pseudo-time factor was employed to effectively linearize the partial differential equations of the unsteady flow response. The production performance of vertically fractured wells in shale gas reservoirs under either constant flow rate or constant bottom-hole pressure conditions was analyzed using the composite flow model. The calculation results indicate that the non-linearities that develop in the gas diffusivity equation have significant effects on the unsteady response, leading to a larger pressure depletion and rate decline in the late-time period. In addition, gas desorption from the shale acts as a recharge source, which relieves the gas production rate of decline. Greater values for the Langmuir volumes or Langmuir pressures provide additional pressure support, leading to a lower rate decline while the flowing well bottom-hole pressure is maintained. The reservoir size mainly affects the duration of the pressure depletion and rate decline. In the case of ignoring the non-linearity and adsorption-desorption effect in the differential equation, a greater rate decline under constant bottom-hole pressure production can be obtained during the boundary-dominated depletion. This work provides a better understanding of gas desorption in shale gas reservoirs and new insight into investigating the production performances of fractured gas well.

Keywords: non-linear differential equation; shale gas; vertically fractured well; composite flow model; adsorption-desorption effect

1. Introduction

In recent years, shale gas reservoirs have gradually become the major sources of natural gas production around the world. In nature, shale can serve as both source and reservoir rock [1–3], and natural gases are stored in both the free gas and absorbed gas forms. Martin et al., stated that the amount of shale gas in place is controlled by the total organic contents (TOC), clays, and adsorption ability of methane on the internal surface of a solid [4]. In shale reservoirs, gas desorption can produce a considerable amount of gas. Tinni et al., presented a novel approach that can be used to evaluate the influence of adsorption on the gas production in shale gas reservoirs [5]. The production performances can be altered by the influence of gas adsorption in unconventional reservoirs [6]. Mengal and Wattenbarger concluded that it is generally not possible to investigate the accurate production forecasts if the effects of desorption is neglected [7]. Thompson et al. [8] proposed that gas desorption can have a great influence on the analysis of conventional Arps decline curves [9]. Recently, much of the research has focused on the adsorption-desorption effect in unconventional reservoirs [10–15]. Since

a portion of the gas in shale reservoirs is stored in the adsorbed form, a detailed investigation on the contribution of gas adsorption can provide critical insights into the analysis of the transient flow behavior in gas reservoirs.

During the last few decades, increasing attention has been paid to the economical development of shale gas reservoirs using hydraulic fracturing [16–24]. In some cases, the adoption of the composite flow model can replace the application of a two-dimensional or three-dimensional flow model when analyzing the transient performance of a fractured well. In terms of the analysis on a composite flow model, Wattenbarger et al., claimed that the flow near production wells in tight gas reservoirs is dominated by a one-dimensional flow after hydraulic fracturing treatment, and they reported a rate decline analysis of gas wells using a one-dimensional flow model [25]. Cinco et al., performed an appropriate analysis of fractured wells according to the bilinear flow theory for the early-time pressure behavior [26]. Later, Cinco and Satnaniago proposed a new approach to analyze the pressure transient response of a vertical fractured well [27]. Brown et al., established an analytical trilinear flow model to investigate the production performance of a fractured well in an unconventional reservoir [28]. In recent years, the composite flow models have been applied to analyze the production performance of fractured wells [29–33]. Stalgorova et al., established an analytical model, as an extension of the trilinear flow solution, for unconventional reservoirs with multiply-fractured horizontal wells [34,35]. Yao et al., established a semi-analytical composite model for heterogeneous reservoirs [36]. Guo et al., presented an analytical model for the production decline analysis of a multi-stage fractured shale reservoir [37]. However, the significant influences of fluid properties changes on the fracture performance were not fully investigated in these studies.

Since the recent boom in gas production caused by the development of hydraulic fracturing technologies, many articles analyzing the transient performance of gas flow in unconventional reservoirs have been published [38–41]. A historical challenge in gas reservoir analysis is how to solve the highly non-linear gas partial differential equation, which fully considers the significant changes in gas properties during depletion. Overall, many researchers [42–49] have focused on the application of pseudo-functions to achieve the linearization and subsequent analytical treatment of the gas flow equations, replacing the pressure and time variables with pseudo-pressure and pseudo-time functions. With this method, the change in gas properties during production is also taken into consideration. On this basis, the main objective of this article is to explore the applicability of the pseudo-functions approach, which investigates the variable gas properties and significant desorption effect in shale gas reservoirs. Firstly, the extended pseudo-function is applied into a composite flow model to obtain the analytical solution. Then, type curves are constructed to analyze the effects of the fluid properties, gas desorption and reservoir size on the transient behaviors. The pseudo-time factor is employed to effectively linearize the partial differential equations of unsteady gas flow in shale gas reservoirs.

2. Pseudo-Functions Approach

2.1. Derivation of the Pseudo-Functions

The presence of adsorbed phases significantly affects the production performance and reserve evaluation of a shale gas reservoir. Consequently, the pressure depletion rapidly increases with the process of gas production in the late-time period, and it is necessary to take the adsorption-desorption effect into consideration. The equilibrium between adsorbed phase and the solid phase at a given pressure is characterized by an adsorption isotherm. Sing et al., presented the detailed description of the six models of physical sorption isotherms [50]. There are also other types of adsorption isotherm models that have been applied to analyze the sorption data in the experimental process, such as the Freundlich-type isotherm [51] and Dubinin's family of isotherms [52]. However, these isotherm models have not been clearly accepted in analyzing the transient responses of unconventional gas reservoirs.

By far, the adsorption isotherm that has been widespread applied to model the adsorption-desorption effect is the Langmuir isotherm [53] as given in Equation (1):

$$V_g(p) = \frac{V_L p}{p_L + p} \quad (1)$$

where $V_g(p)$ is the gas volume of the adsorption at pressure p ; V_L is the Langmuir volume, referred to as the maximum gas volume of adsorption at an infinite pressure; and p_L is the Langmuir pressure, which is the pressure corresponding to one-half of the Langmuir volume. Based on the equation describing the mass balance of gas flow in shale gas reservoirs proposed by Patzek et al., and Yu et al. [54,55], the one-dimensional continuity equation with the adsorption-desorption effect is given below:

$$-\frac{\partial(\rho_g v_g)}{\partial x} = \frac{1}{\alpha_t} \frac{\partial[\rho_g S_g \phi + (1 - \phi)\rho_a]}{\partial t} \quad (2)$$

where ρ_g is the free gas density; v_g is the Darcy velocity of gas; S_g is the initial gas saturation; ϕ is the reservoir porosity, ρ_a is the adsorbed gas density; and $\alpha_t = 3.6 \times 24 \times 10^{-3}$ is the conversion factor. When neglecting the elasticity of the porous media under isothermal conditions, a nonlinear governing equation for a one-dimensional transient flow with the gas desorption effect in a shale gas reservoir can be presented as:

$$\frac{\partial}{\partial x} \left[\frac{k_g}{\mu_g(p)} \cdot \frac{p}{Z(p)} \frac{\partial p}{\partial x} \right] = \frac{1}{\alpha_t} \left[\phi S_g + (1 - \phi) \frac{\partial \rho_a}{\partial \rho_g} \right] \frac{\partial}{\partial t} \left(\frac{p}{Z(p)} \right) \quad (3)$$

where k_g is the reservoir permeability, μ_g is the gas viscosity, and Z is the gas compressibility factor.

As given in Equation (3), the viscosity $\mu_g(p)$ and compressibility factor $Z(p)$ are pressure-dependent parameters of natural gas, and Equation(3) is apparently nonlinear. In order to solve this nonlinear equation, the pseudo-pressure function [56] is defined as follows:

$$p_p(p) = \frac{\mu_{gi} Z_i}{p_i} \int_p^{p_i} \frac{p}{\mu_g(p) Z(p)} dp \quad (4)$$

where p_p is the pseudopressure, μ_{gi} is the initial gas viscosity, Z_i is the initial gas compressibility factor, and p_i is the initial pressure. Substituting the pseudo-pressure function and Langmuir adsorption model into the diffusivity equation, the flow of a real gas through a shale formation can be expressed as follows:

$$\frac{\partial^2 p_p(p)}{\partial x^2} = \frac{\phi \mu_{gi} c_{gi} S_g}{\alpha_t k_g} \left[\frac{\mu_g(p) c_g(p)}{\mu_{gi} c_{gi}} + \frac{\mu_g(p) \rho_b}{\mu_{gi} c_{gi} \phi S_g} \frac{p_{sc} Z(p) T}{p Z(p_{sc}) T_{sc}} \frac{V_L p_L}{(p_L + p)^2} \right] \frac{\partial p_p(p)}{\partial t} \quad (5)$$

where c_{gi} is the initial gas compressibility, c_g is the gas compressibility, ρ_b is the bulk density of shale, and $Z_{sc}(p_{sc})$ is the gas compressibility factor under the standard condition. Due to the residual presence of the $\mu_g(p) c_g(p)$ pressure-dependent term on the right hand side of this diffusivity formulation, it is necessary to implement further handling of the nonlinearity in Equation (5). The traditional method is to approximate it as a constant, which will produce a large error in an analysis of the production performance.

In the initial stage, viscosity-compressibility changes do not dominate the unsteady state responses of the system, and $\mu_g(p) c_g(p)$ is shown to represent a weak non-linearity. This is the same with as the phenomenon in liquid systems. However, the significant changes in $\mu_g(p) c_g(p)$ during the boundary-dominated depletion cannot be ignored in gas reservoirs. In order to investigate the effect of pressure-dependent fluid properties on transient responses, pseudo-variables are needed to be implemented in unsteady state analysis. Recently, Ye and Ayala [57] proposed a density-based

approach to analyze the unsteady state responses for natural gas reservoirs. This approach emphasized the significance of viscosity-compressibility changes from the pressure depletion based on the following depletion-driven dimensionless variables:

$$\beta^*(t) = \frac{1}{t} \int_0^t \frac{\mu_{gi} c_{gi}}{\mu_g(p_{avg}) c_g(p_{avg})} dt \quad (6)$$

where p_{avg} is the average pressure in the reservoir. To effectively linearize the partial differential Equation (5) for the cases under study, pseudo-functions should be applied to re-express the pseudo-variables on the right hand side of the differential equation in a friendlier way. On this basis, according to the results of Fraim [58], the pseudo-time factor considering the adsorption-desorption effect in this work is defined as follows:

$$\beta(t) = \frac{1}{t} \int_0^t \frac{1}{\left[\frac{\mu_g(p_{avg}) c_g(p_{avg})}{\mu_{gi} c_{gi}} + \frac{\mu_g(p_{avg}) \rho_b}{\mu_{gi} c_{gi} \phi S_g} \frac{p_{sc} Z(p_{avg}) T}{p_{avg} Z(p_{sc}) T_{sc}} \frac{V_L p_L}{(p_L + p_{avg})^2} \right]} dt \quad (7)$$

The integrand function $\lambda(t)$ is defined as follows:

$$\lambda(t) = \frac{1}{\left[\frac{\mu_g(p_{avg}) c_g(p_{avg})}{\mu_{gi} c_{gi}} + \frac{\mu_g(p_{avg}) \rho_b}{\mu_{gi} c_{gi} \phi S_g} \frac{p_{sc} Z(p_{avg}) T}{p_{avg} Z(p_{sc}) T_{sc}} \frac{V_L p_L}{(p_L + p_{avg})^2} \right]} \quad (8)$$

Apparently, $\lambda(t)$ and $\beta(t)$ are dimensionless and the relationship between them can be presented as follows:

$$\beta(t) = \frac{1}{t} \int_0^t \lambda(t) dt \quad (9)$$

Substituting the pseudo-function variable into the diffusivity Equation (5), the simplified version of the governing equation is shown below:

$$\frac{\partial^2 p_p(p)}{\partial x^2} = \frac{\phi(1 - S_{wi}) \mu_{gi} c_{gi}}{\alpha_t K_g} \frac{\partial p_p(p)}{\partial (\beta t)} \quad (10)$$

where $\beta(t)$ is a depletion-driven time rescaling factor capturing the behavior of the gas desorption and viscosity-compressibility changes during pressure depletion. It should be noted that Equation (10) is an approximate version of Equation (3). The proposed approximation demonstrates that the introduction of the pseudo-time factor can successfully linearize the partial differential equation of the gas flow in porous media, making the analysis methods for the “liquid flow model” applicable to the gas flow in a shale reservoir.

2.2. Behaviors of the Pseudo-Time Factor

On the basis of the proposed approach, this section demonstrates the effects of the pseudo-time factor during reservoir depletion. Apparently, the behaviors of the pseudo-time factor over time depend on the correlated fluid properties and depletion patterns in the system. A full discussion of the production performances for these cases under study is presented using the production decline model of one-dimensional flow [25]. Consider a vertical well intercepted by a uniform flux vertical fracture in the center of a homogeneous rectangular reservoir, as shown in Figure 1. The height, length, and width are h , x_e , and y_e , respectively. The half-length of the fracture is y_f , and the length of the fracture is equal to the width of the reservoir.

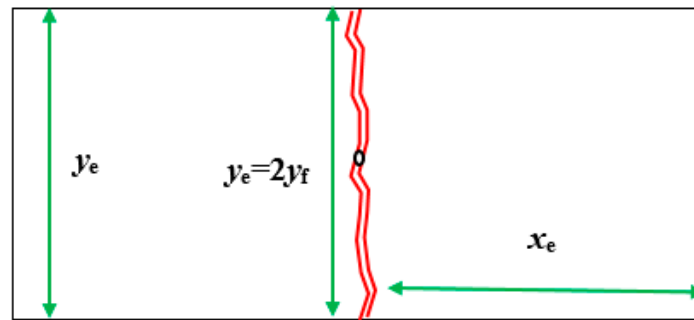


Figure 1. Diagram of one-dimensional fluid flow.

If the fracture produces at a pressure of p_{wf} , this leads to isothermal transient flows in the reservoir. The dimensionless quantities are defined as follows:

$$p_D = \frac{p_P(p)}{p_P(p_{wf})}, q_D = \frac{q_g(t)\mu_{gi}B_{gi}}{\alpha_p k_g h p_P(p_{wf})}, t_{Df} = \frac{\alpha_t k_g t}{\phi(1 - S_{wi})\mu_{gi}c_{gi}y_f^2}, x_D = \frac{x}{y_f}$$

where q_g is the gas flow rate, B_{gi} is the gas formation volume factor under the standard condition, h is the reservoir thickness, p_{wf} is the wellbore pressure, y_f is the fracture half-length, and $\alpha_p = 2\pi \times 3.6 \times 24 \times 10^{-7}$ is the conversion factor. In these equations, p_D is the dimensionless pseudo pressure, q_D is the dimensionless flow rate, t_{Df} is the dimensionless time, and x_D is the dimensionless coordinate in the x direction. The production behavior under a constant bottom-hole pressure is given below:

$$q_D(\beta t_{Df}) = \frac{4}{\pi x_{eD}} \sum_{n=0}^{\infty} \exp\left[-\frac{\pi^2}{4}(2n+1)^2 \frac{(\beta t_{Df})}{x_{eD}^2}\right] \quad (11)$$

where x_{eD} is the dimensionless reservoir length. In this formulation, the calculation of depletion-driven factor $\beta(t)$ should be explicitly stated.

It should be noted that high accuracy can be obtained from Equation (7) by employing the material balance equation with the adsorption-desorption effect. A generalized material balance equation that investigates the equilibrium between the free and adsorbed gas phases was developed by King [59], who applied graphical and iterative algorithms for the solution of the generalized results. Since then, based on the volume conservation principle, Moghadam et al., presented a new format for the material balance equation accounting for the shale gas storage mechanisms [60]. In this paper, the material balance equation with the adsorption-desorption in a shale gas reservoir has been derived by integrating the continuity equation with definite conditions.

The definite conditions for Equation (2) are presented as follows:

$$(\rho_g v_g)_{x=0} = -\frac{q_{gsc}(t)\rho_{sc}}{\alpha_p h w}, (\rho_g v_g)_{x=x_e} = 0, (q_{gsc})_{t=0} = 0$$

where q_{gsc} is the standard gas flow rate, and ρ_{sc} is the gas density under the standard condition. Then, the one-dimensional continuity equation with the adsorption-desorption effect in integral form is given by the following:

$$-\frac{1}{x_e} \int_0^{x_e} \frac{\partial(\rho_g v_g)}{\partial x} dx = \frac{1}{\alpha_t} \frac{1}{x_e} \int_0^{x_e} \frac{\partial[\rho_g S_g \phi + (1 - \phi)\rho_a]}{\partial t} dx \quad (12)$$

Substituting the Langmuir isotherm model into the continuity Equation (12), the material balance equation considering the gas desorption in a shale gas reservoir is given below:

$$\frac{G_p(t)}{G_{sc}} \frac{p_i}{Z_i} = \left(\frac{p_i}{Z_i} - \frac{p_{avg}}{Z_{avg}} \right) + \frac{p_{sc} T_i}{Z_{sc} T_{sc}} \frac{\rho_b V_L}{\phi S_{gi}} \left[\frac{p_i}{p_L + p_i} - \frac{p_{avg}}{p_L + p_{avg}} \right] \tag{13}$$

where G_p is the cumulative production, and G_{sc} is the geological reserves.

The time-dependence of $\beta(t)$ is correlated with the associated average reservoir pressure p_{avg} predicted by the material balance equation at every depletion step for every value of $G_p(t)$. For a reservoir with a constant flow rate, the cumulative production is $G_p = q_{sc} \times t$. If the well has variable rate production, the trapezoidal numerical integral can be incorporated to obtain the accumulative production for a given time.

At every step in the isothermal depletion process, reservoir fluid properties such as the gas compressibility, viscosity, and gas volume of adsorption can be readily tracked as functions of the pressure and time. According to the definition of the pseudo-time factor in this work, which decouples the viscosity-compressibility changes and gas desorption from the pressure depletion in a shale gas reservoir, the transient response of a shale gas reservoir can be further analyzed. Based on the above derivation, the behaviors of pseudo-time factors $\beta(t)$ and $\beta^*(t)$ can be calculated according to the isothermal depletion of a stated reservoir, as shown in Figure 2. On this basis, the production performances of liquid and gas solutions can be investigated by calculating Equation (11) with the use of Stehfest numerical inversion algorithm [61] (Figure 3).

Figure 2 depicts the curves of $\beta(t)$ and $\beta^*(t)$ versus time with different reservoir sizes under a constant bottom-hole pressure. As shown in this figure, in the initial stage, the extent of reservoir depletion is not significant, that is $\beta^*(t) \approx 1.0$. The viscosity-compressibility changes have a weak effect on the unsteady state responses of the system. At a later production stage, the average reservoir pressure p_{avg} decreases sharply, and the seepage behavior in the gas reservoirs would gradually deviate from that of its corresponding liquid system ($\beta^*(t) < 1.0$). As the production time increases, the desorption effect on the reservoir pressure depletion is significant, which indicates that a recharge source has been built in a shale gas reservoir. The deviation between the seepage behavior in a shale gas reservoir and that of its corresponding liquid system, at a later production period, becomes more significant.

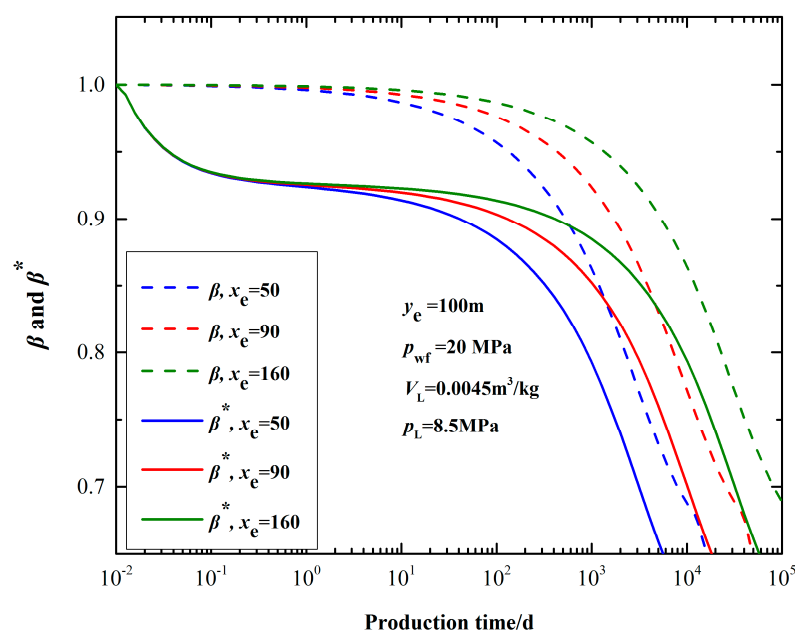


Figure 2. Change relationship of $\beta(t)$ and $\beta^*(t)$ over time.

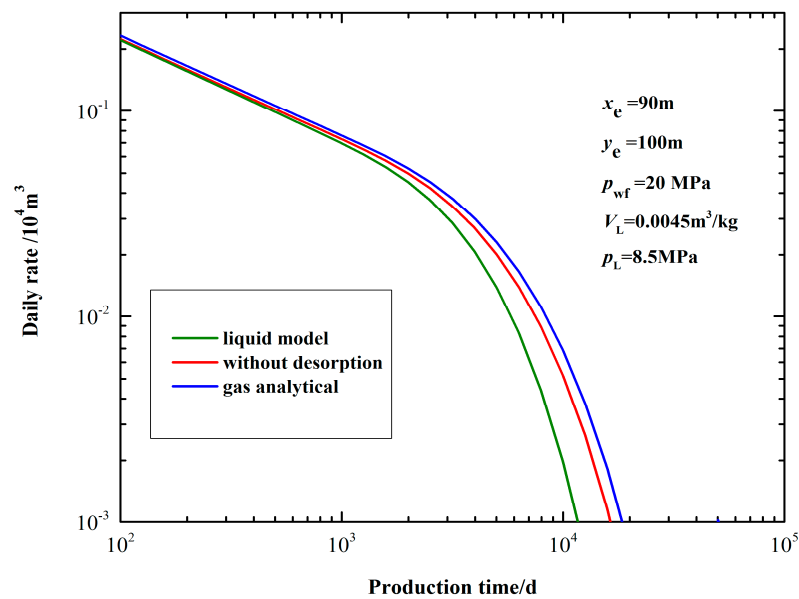


Figure 3. Influences of depletion-driven fluid properties and gas desorption on gas production with one-dimensional flow model.

The impact of the gas desorption on production rate under a constant bottom-hole pressure is presented in Figure 3. As shown in this figure, at an early stage, the production rates simulated using the liquid model, and the gas model with and without desorption model, are very similar. This is because the reservoir depletion is small and cannot significantly affect the viscosity-compressibility values of natural gas. However, during the later production period, the gas responses gradually deviate from their corresponding liquid analytical model results. Thus, the production rate of a shale gas reservoir is higher than that of a slightly-compressible liquid reservoir. It should be noted that the flow rate decreases as the production time increases, while the bottom-hole pressure is maintained and production behaviors are significantly affected by the depletion-driven fluid properties and gas desorption in a shale gas reservoir. For the flow in the liquid analytical model, the adsorption-desorption effect and significant changes in the gas properties during depletion are neglected, and the rate declines faster than under the other two conditions. This is explained by the significant changes in the fluid properties during the reservoir depletion. In addition, the desorption effect of shale gas is equivalent to an energy supply in the reservoir. Consequently, if the gas desorption is not considered, the conventional gas model would underestimate the later stage production rate under a bottom-hole pressure condition.

3. Mathematical Model

In this article, an analytical solution is presented to characterize the production performance of a fractured well in a shale gas reservoir. The composite flow model is simple, but flexible enough to embody the basic properties of an unconventional reservoir. For a gas reservoir, especially one with a relatively narrow drainage area, a composite flow model is an appropriate method to avoid the need to solve integral equations and analyze the transient flow in a finite-conductivity fracture coupled with the reservoir flow. One of the best advantages of the composite model is that it is convenient to derive the approximate solutions. Based on the above results, the production performance of a vertically fractured well in a shale gas reservoir under either constant flow rate or constant bottom-hole pressure conditions can be obtained by using the trilinear flow model.

3.1. Model Assumption

Assuming that a finite-conductivity fractured well with a bi-wing shape is completed in a homogeneous rectangular gas reservoir; its length, width, and height are x_e , y_e , and h respectively. The case of a slab transverse vertical fracture in the center of the reservoir is examined, where the height of the fracture is equal to the thickness of the reservoir. The shale gas flows into the wellbore from the reservoir through the fracture. It is assumed that the well produces at a constant flow rate, and an isothermal seeping process appears in the reservoir. Take the lower left corner of the gas reservoir as the origin of the coordinates $(0, 0)$, as shown in Figure 4.

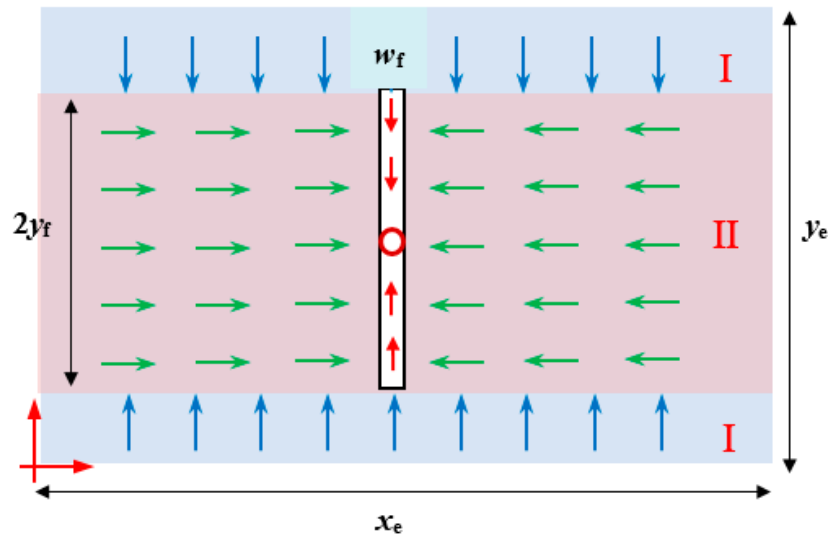


Figure 4. Diagram of composite flow model for vertically fractured well.

The dimensionless quantities are defined as follows:

$$p_{ID} = \frac{p_D(p_I)}{p_P(p_{wf})} \quad p_{IID} = \frac{p_P(p_{II})}{p_P(p_{wf})} \quad p_{fD} = \frac{p_P(p_f)}{p_P(p_{wf})},$$

$$y_D = \frac{y}{y_f} \quad y_{eD} = \frac{y_e}{y_f} \quad y_{fD} = \frac{y_f}{y_f} \quad w_{fD} = \frac{w_f}{y_f} \quad c_{fD} = \frac{k_f w_f}{k y_f}$$

where y_D is the dimensionless coordinate in the y direction, y_{eD} is the dimensionless reservoir width, y_e is the reservoir width, w_{fD} is the dimensionless fracture width, w_f is the fracture width, c_{fD} is the dimensionless fracture conductivity, k_f is the fracture permeability, and w_f is the fracture width.

3.2. Solution for the Model

Referring to the definition of pseudo-time factor $\beta(t)$ that has been presented in this paper, the dimensionless governing equation for the gas flow in the formation is as follows. Detailed derivation of the mathematical model is presented in Appendix A:

$$\frac{\partial^2 p_D}{\partial x_D^2} + \frac{\partial^2 p_D}{\partial y_D^2} = \frac{\partial p_D}{\partial (\beta t_D)} \quad (14)$$

(1) In Region I, the linear flow is parallel to the surface of the fracture (y -direction), and Equation (14) is simplified as follows:

$$\frac{\partial^2 p_{ID}}{\partial y_D^2} = \frac{\partial p_{ID}}{\partial (\beta t_{Df})} \quad (15)$$

(2) The flow in the reservoir is mainly the linear flow vertical to the surface of the fracture in Region II (dominated by that in the x -direction).

$$\frac{\partial^2 p_{IID}}{\partial x_D^2} + \frac{1}{y_{fD}} \frac{\partial p_{ID}(x_D, \frac{1}{2}y_{eD} + y_{fD}, \beta t_{Df})}{\partial y_D} = \frac{\partial p_{IID}}{\partial(\beta t_{Df})} \quad (16)$$

(3) The governing equation can be calculated by the integral average along the x direction (the pressure function is still denoted as p_{fD}), and the corresponding dimensionless governing equation is as follows:

$$\frac{d^2 p_{fD}}{dy_D^2} + \frac{2}{c_{fD}} \frac{\partial p_{IID}(\frac{1}{2}x_{eD} + \frac{1}{2}w_{fD}, y_D, \beta t_{Df})}{\partial x_D} = 0 \quad (17)$$

The pressure distribution function of a vertical fracture under a constant flow rate in the Laplace domain is obtained as follows:

$$s\tilde{p}_{fD}(y_D, s) = \frac{\pi}{c_{fD}} \frac{1}{\sqrt{D(s)}} \frac{\cosh(y_D - \frac{1}{2}y_{eD} - y_{fD})\sqrt{D(s)}}{\sinh y_{fD}\sqrt{D(s)}} \quad (18)$$

where s is the time variable in Laplace domain. The relationship between the pressure solution at a constant rate and the flow rate solution under a constant bottom-hole pressure can be derived according to the superposition principle [62]:

$$\tilde{p}_D(s) \cdot \tilde{q}_D(s) = \frac{1}{s^2} \quad (19)$$

where \tilde{p}_D is dimensionless pseudo pressure p_D of finite-conductivity fracture in Laplace domain, \tilde{q}_D is dimensionless flow rate q_D of finite-conductivity fracture in Laplace domain. Then, they can be inverted to the real domain numerous times by the use of an algorithm (such as that of the Stehfest numerical inversion) during the integration over the time and spatial domains.

3.3. Model Validation

As shown in Figure 5, the solution proposed in this paper was validated using HIS Fekete Harmony [63], which can provide solutions to support customers in various gas well production analysis and simulation services [64,65]. The composite method was applied to model the gas flow in a shale gas reservoir. The reservoir was assumed to be homogeneous. The reservoir had a finite length of 1200 m and width of 800 m. The value of the bottom-hole pressure was held at 10 MPa for the simulation. The fracture height was supposed to be equal to the formation thickness (47.2 m). The fracture half-length was fixed at 70 m. The adsorption effect was characterized by the Langmuir isotherm. The comparison suggested that there was a good agreement between the solutions derived in this article and the results from commercial software. Thus, the results validated the accuracy of our model.

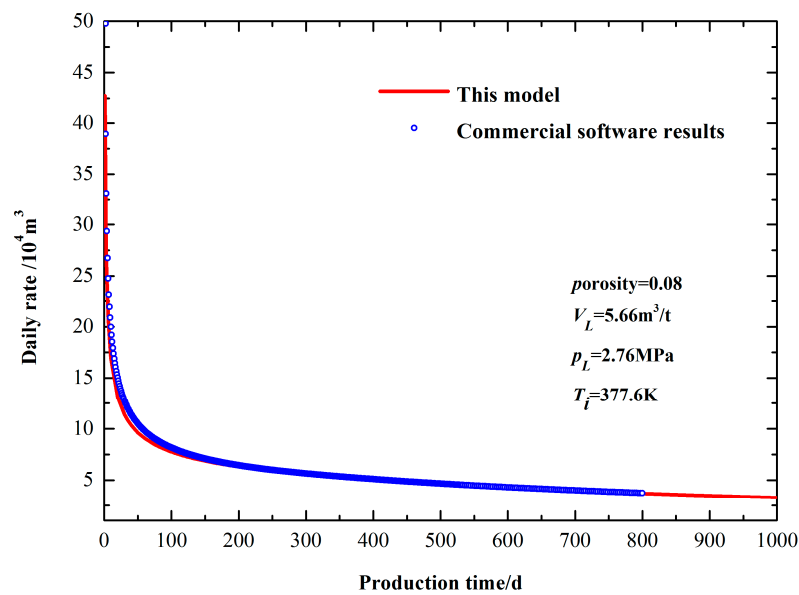


Figure 5. Comparison of flow rate results of this model and commercial software.

4. Parametric Study on Type Curves

The dynamic characteristics under constant flow rate or constant bottom-hole pressure condition can be derived by illustrating the influence of the depletion-driven fluid properties and gas desorption in a shale gas reservoir. The comparison of the liquid and gas analytical solutions can be derived correspondingly. The fractured well, fluid, and formation properties associated with the generation of the type curves are listed in Table 1.

Table 1. Data used in discussion.

Parameter	Value	Unit
k_g	0.0008	$10^{-3} \mu\text{m}^2$
ϕ	14	%
S_{wi}	10	%
h	25	m
γ_g	0.6	Value
y_f	50	m
p_i	34.5	MPa
T_i	327.6	K
ρ_b	2.63×10^3	kg/m^3
c_{fD}	1.5	Value

4.1. Effects of Depletion-Driven Fluid Properties and Gas Desorption

The effects of the depletion-driven fluid properties and gas desorption on the pressure depletion for a vertically fractured well under a constant flow rate are presented in Figure 6. As shown in this figure, in the initial stage, the curves agree well with each other. At a later production period, the curves bend upward, and the effects of the depletion-driven fluid properties and gas desorption on the curves become more significant. When neglecting the adsorption-desorption effect and significant changes in the gas properties during depletion, a greater pressure drop would be required to maintain the expected flow rate. As a result, the pressure depletion is closer to reality when considering the effects of the gas property changes and gas desorption during reservoir depletion, and provides extra information on shale gas production. The impact of the reservoir size on the pressure response under a constant flow rate is also shown in Figure 6. As expected, a larger pressure difference is required

to maintain a constant flow rate in a smaller size reservoir; it also illustrates that a closer boundary distance is associated with a quicker appearance of an upward trend.

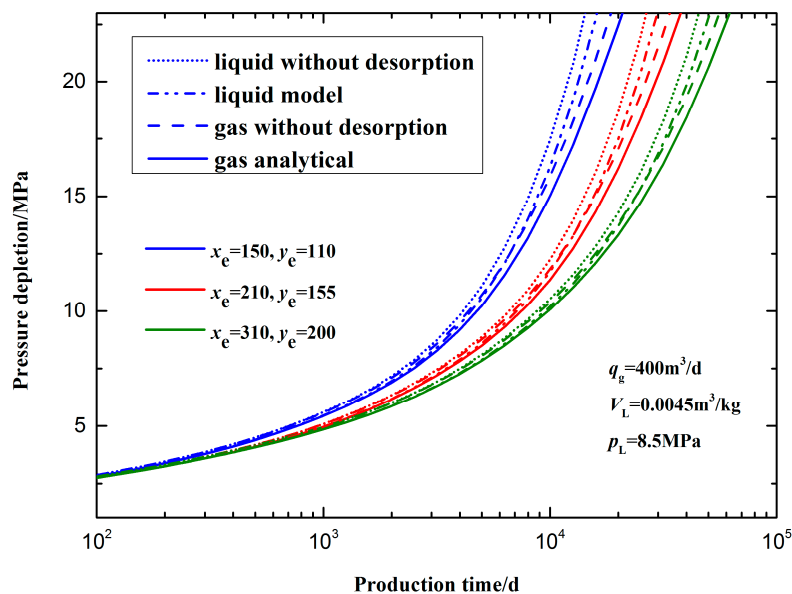


Figure 6. Effects of depletion-driven fluid properties, gas desorption, and outer boundary on pressure behavior.

Figure 7 illustrates the impact of the depletion-driven fluid properties, gas desorption and reservoir size on the production behaviors under a constant bottom-hole pressure condition. As presented in this figure, in the early stage, the curves agree with each other. The flow rate decreases as the production time increases, while the flowing well bottom-hole pressure is maintained, and production behaviors can be significantly affected by the fluid property changes and gas desorption. For the flow in a liquid analytical model, the significant changes of in the gas properties during depletion are neglected, leading to a larger rate decline and smaller cumulative production. These results are compared in this figure against the analytical trilinear flow solution of Brown and Ozkan [28], which did not incorporate fluid properties corrections. In another case, a larger rate decline and smaller cumulative production can be obtained when neglecting the desorption effect. These results are compared in the same figure against the unmodified density-based solution of Ye and Ayala [57], which did not incorporate desorption corrections, yielding a poor prediction. For example, for a reservoir with a length of 150 m and width of 110 m, the rigorous solution predicts a rate decline from 8700 to 1000 m³ in 6.46 years. If the non-linearity is neglected in the differential equation, this decline in the flow rate is predicted to occur in 5.68 years; if the solution is derived without considering gas desorption, this decline in flow rate is predicted to occur in 5.9 years. At 15 years of production, the cumulative production values for the above two cases are calculated with errors of 6.7% and 4.2%, respectively. It is worth noting that changes in the fluid properties and gas desorption have a significant influence on gas production in the late-time period. Figure 7 also presents the rate decline curves with different reservoir sizes under a constant bottom-hole pressure condition. It can be seen that the reservoir size has a dominant effect in the later production period, and a larger reservoir would lead to a later downward trend.

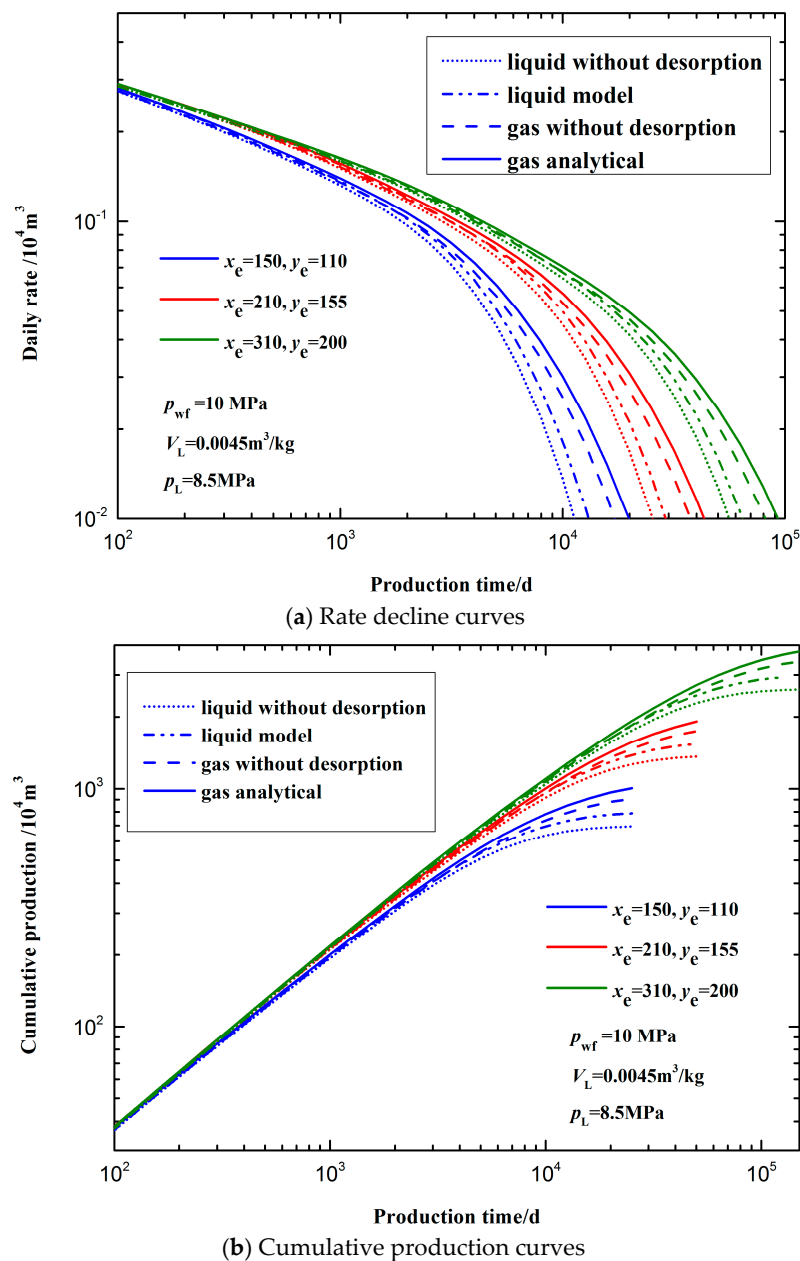
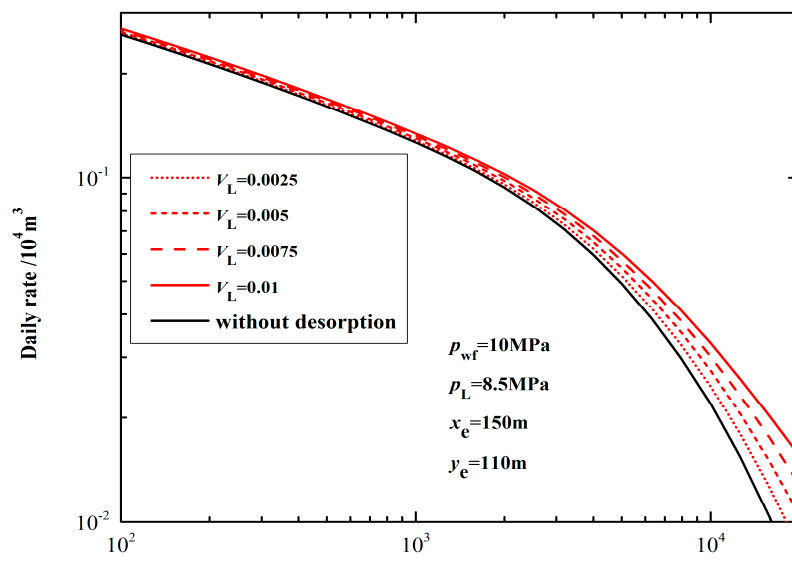


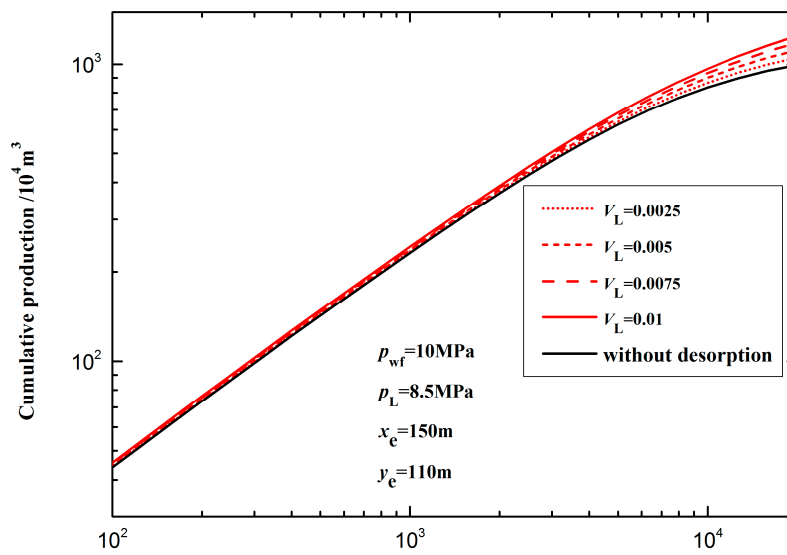
Figure 7. Effects of depletion-driven fluid properties, gas desorption, and outer boundary on production behavior.

4.2. Effect of Langmuir Volume

Figure 8 shows the effect of the Langmuir volume on the production behavior under a constant bottom-hole pressure condition. For the reservoir with a certain amount of gas content, under the same pressure condition, a larger Langmuir volume value leads to a greater adsorption capacity in a shale gas reservoir. Due to the presence of adsorbed gas, the gas reservoir can receive support from the additional gas source, which leads to larger gas production in shale gas reservoirs. As shown in this figure, the effect of desorption is minimal at early times. As the depletion progresses, greater Langmuir volumes lead to additional pressure support, and thus less rate decline and larger cumulative production while the flowing well bottom-hole pressure is maintained. When ignoring the adsorption-desorption effect of shale gas, a greater rate decline will appear under a constant bottom-hole pressure.



(a) Rate decline curves



(b) Cumulative production curves

Figure 8. Effects of Langmuir volume value on production behavior.

Figures 9 and 10 show the effects of the Langmuir volume on pseudo-time variables $\beta(t)$ and $\lambda(t)$ under a constant bottom-hole pressure condition. Due to the presence of adsorbed gas, the gas reservoir can receive support from the additional gas source. As a result, the changes in the Langmuir volume can significantly affect the behaviors of $\beta(t)$ and $\lambda(t)$. Greater Langmuir volumes provide additional pressure support leading to lower $\beta(t)$ and $\lambda(t)$ values.

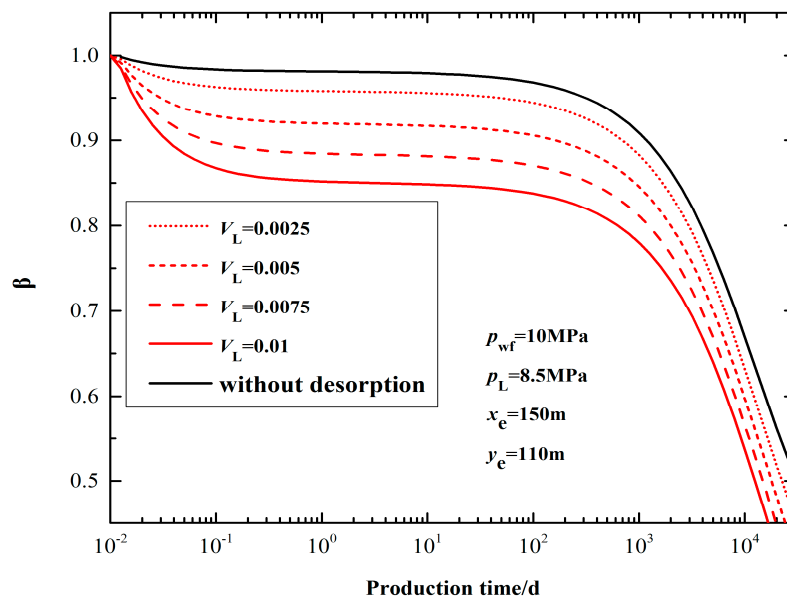


Figure 9. Effects of Langmuir volume on pseudo-time factor $\beta(t)$.

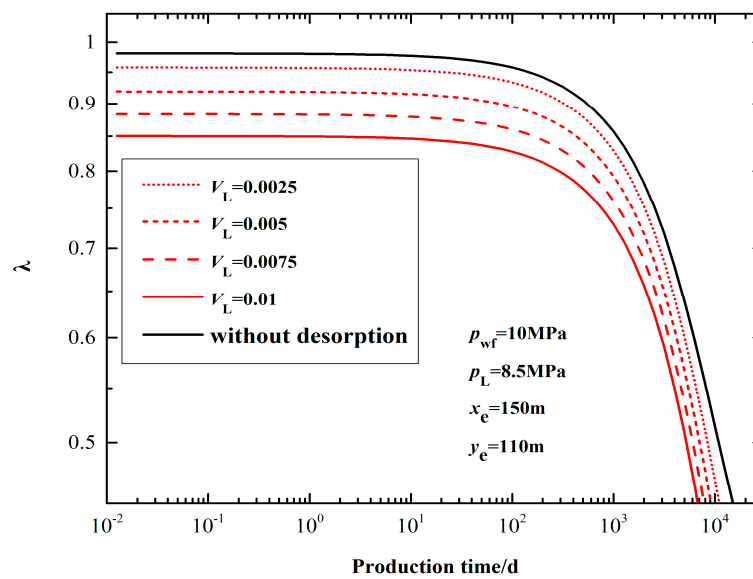
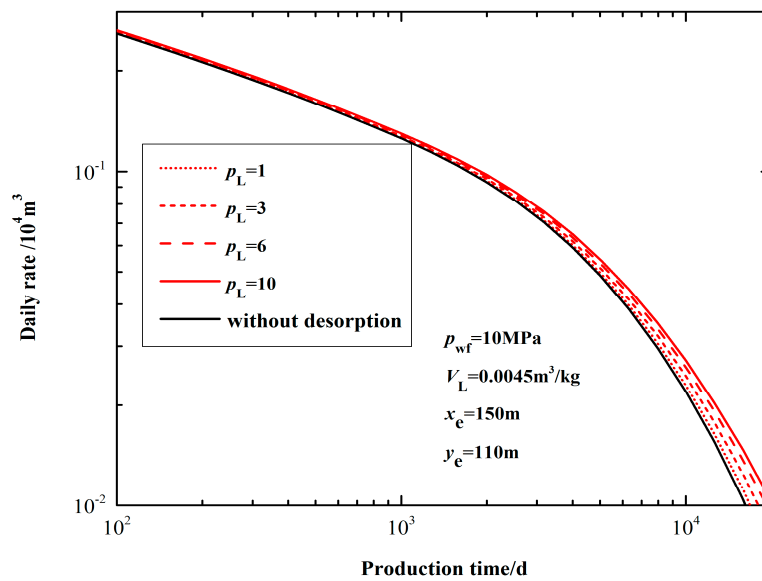


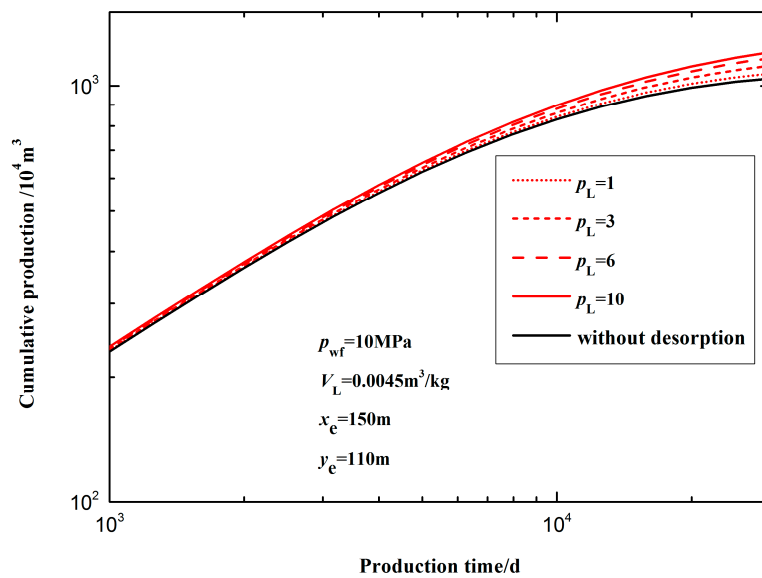
Figure 10. Effect of Langmuir volume on pseudo-time variable $\lambda(t)$.

4.3. Effect of Langmuir Pressure

Figure 11 shows the effect of the Langmuir pressure on the production behavior under a constant bottom-hole pressure condition. In a shale gas reservoir, the Langmuir pressure is used to characterize the adsorption capacity of the reservoir, which is related to the nature and temperature of the reservoir and gas. As shown, the effect of desorption is minimal at early times. As the depletion progresses, greater Langmuir pressures will lead to a smaller rate decline and larger cumulative production while the flowing well bottom-hole pressure is maintained. If the adsorption-desorption effect is neglected, a greater rate decline will appear under the constant bottom-hole pressure condition.



(a) Rate decline curves



(b) Cumulative production curves

Figure 11. Effects of Langmuir pressure value on production behavior.

Figures 12 and 13 show the curves of $\beta(t)$ and $\lambda(t)$ versus time with Langmuir pressure values under a constant bottom-hole pressure, respectively. The desorption effect of shale gas can provide an additional source of support for the reservoir. As a result, changes in the Langmuir pressure can significantly affect the behaviors of $\beta(t)$ and $\lambda(t)$. Greater Langmuir pressures will lead to lower $\beta(t)$ and $\lambda(t)$ values. It should be noted that production behavior can be affected by gas desorption in shale gas reservoirs.

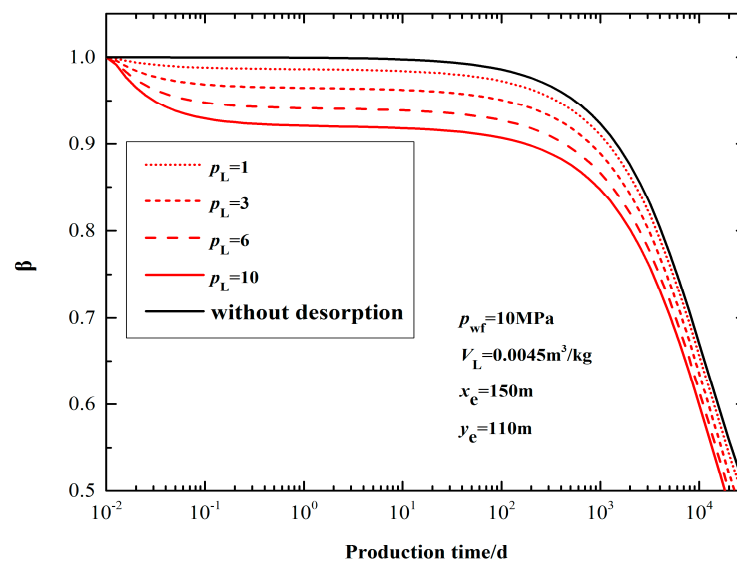


Figure 12. Effects of Langmuir pressure on pseudo-time factor $\beta(t)$.

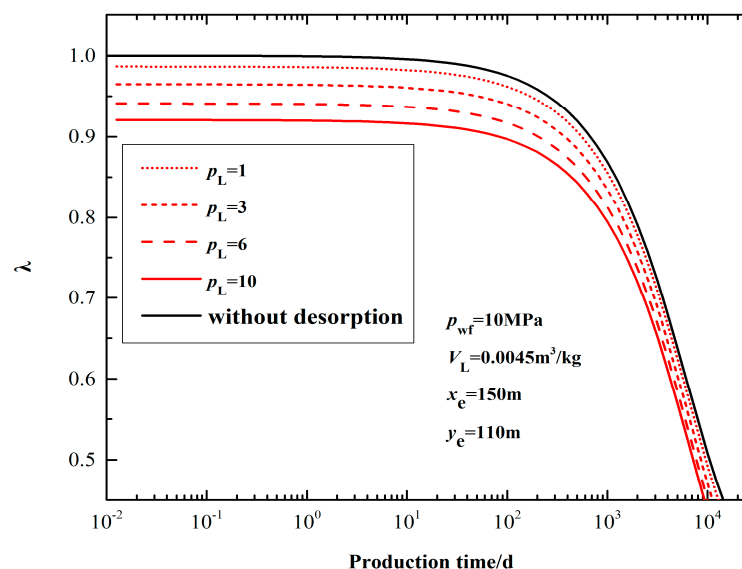


Figure 13. Effects of Langmuir pressure on pseudo-time variable $\lambda(t)$.

4.4. Example Calculation

In this paper, we attempt to apply the analytical solutions to the transient performance of a hydraulic fractured shale gas well in a Sichuan field. The daily rates from the early years have been used for plots. The available reservoir and fracture parameters are listed in Table 2. The gas flow rate is characterized by a decreasing trend for a long time. This indicates that the shale gas is produced with a constant bottom-hole pressure. Figure 14 depicts a log-log decline curve for the transient responses of this example well. The production data has been further applied in type-curve matching that can provide a quick estimation for reservoir and fracture properties, such as the formation permeability, fracture conductivity, and fracture half-length. The best match of the data with the type curve can be obtained by determining the key parameters from those match points in Figure 14. The formation permeability interpreted by our model is 0.0023 mD, and the value of fracture conductivity is 450.6 in the interpretation of matching results. Besides, the fracture half-length calculated by the solutions in this work (48.25 m) can have a good agreement with the designed half-length (45 m), which can further

indicate the accuracy of our model. For this well, we require a further analysis and confirmation because the decline curve can be affected by the potential variation of the pressures and flow rates. In spite of this, the decline curve is considered to be a practical and convenient method to analyze our example well.

Table 2. Reservoir and fracture data.

Parameter	Value	Unit
Initial pressure p_i	16.3	MPa
Initial temperature T_i	338.15	K
Formation thickness h	39.7	m
Porosity ϕ	5	%
Water saturation S_{wi}	34.75	%
Bottom-hole pressure P_{wf}	4.82	MPa
Langmuir volume V_L	3	m^3/t
Langmuir pressure p_L	2.8	MPa
Initial gas compressibility c_{gi}	0.0592	MPa^{-1}
Designed fracture half-length y_f	45	m

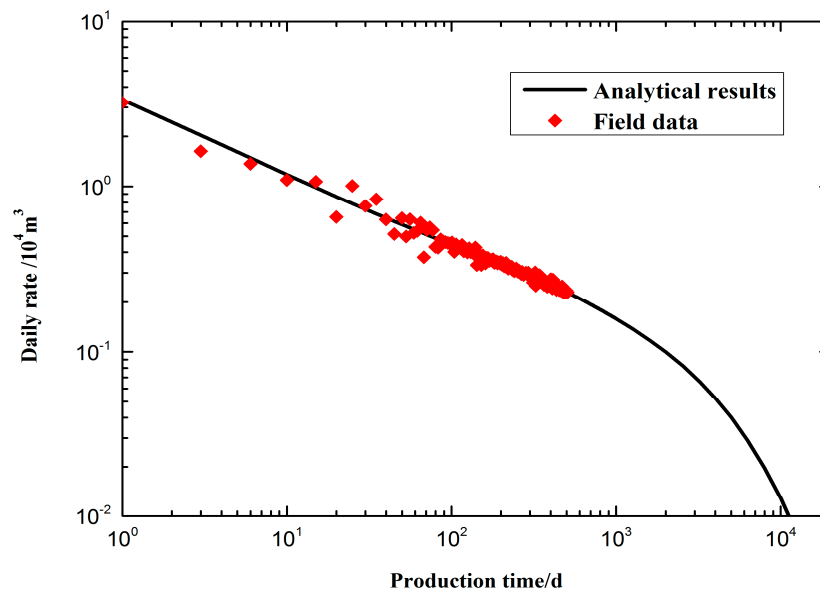


Figure 14. Log-log decline curve for field example.

5. Conclusions

In this article, we established a mathematical model for a fractured well in a shale reservoir that accounted for the non-linearities and desorption effects in partial differential equations. The detailed conclusions based on our work are summarized as follows:

- (1) In this work, the application of the pseudo-functions approach has been extended to solve the nonlinear flow problems of shale gas. This is accomplished by the definition of the pseudo-time factor accounting for both the viscosity-compressibility changes and desorption effect during reservoir depletion. The best advantage of this approach is that some partial differential equations can be effectively linearized, which contributes to the comprehensive investigation of the production performance of a fractured well in a shale gas reservoir.
- (2) The material balance equation with gas desorption is derived by the integration of the continuity equation with definite conditions, which can be used to obtain the analytical results of material balance equation in the application of well testing.

- (3) The modified formulation is validated and verified with the commercial software, and the successful analytical match demonstrates that the proposed model can effectively capture the production performance of gas reservoirs with significant desorption effect.
- (4) At a later production period, the production behaviors are significantly affected by the depletion-driven fluid properties and gas desorption in a shale gas reservoir. The shale gas reservoir can receive support from desorption effect in this period. A larger Langmuir volume or larger Langmuir pressure leads to a greater energy supply and less rate decline under a constant bottom-hole pressure condition.

Acknowledgments: This article was supported by the Fundamental Research Funds for the Central Universities. The careful reviews and detailed comments by the anonymous reviewers and editors are greatly appreciated.

Author Contributions: Xiaodong Wang proposed this topic and supervised the work. Xiaodong Wang and Xiaoyang Zhang were in charge of model establishment and analytical solution. Xiaochun Hou and Wenli Xu analyzed the data. Xiaoyang Zhang wrote the paper.

Conflicts of Interest: The authors declare no conflict of interest.

Nomenclature

Dimensionless Variables

vt_{Df}	dimensionless time
p_D	dimensionless pseudo pressure
q_D	dimensionless flow rate
c_{fD}	dimensionless fracture conductivity
x_D	dimensionless coordinate in the x direction
y_D	dimensionless coordinate in the y direction
x_{eD}	dimensionless reservoir length
y_{eD}	dimensionless reservoir width
w_{fD}	dimensionless fracture width
s	time variable in Laplace domain, dimensionless
\tilde{p}_D	dimensionless pseudo pressure p_D of finite-conductivity fracture in Laplace domain
\tilde{q}_D	dimensionless flow rate q_D of finite-conductivity fracture in Laplace domain

Field Variables

x, y	plane coordinates
w_f	fracture width, m
y_f	fracture half-length, m
x_e	lateral boundary of reservoir, m
y_e	vertical boundary of reservoir, m
p	pressure, MPa
p_i	initial pressure, MPa
p_{wf}	bottom-hole producing pressure, MPa
p_f	fracture pressure, MPa
p_L	Langmuir pressure, MPa
p_p	pseudo pressure, MPa
p_{avg}	average pressure in reservoir, MPa
T_i	temperature in reservoir, K
q_g	gas flow rate, $10^4 \text{ m}^3/\text{d}$
q_{gsc}	standard gas flow rate, $10^4 \text{ m}^3/\text{d}$
k_g	gas reservoir permeability, $10^{-3} \mu\text{m}^2$
k_f	fracture permeability, $10^{-3} \mu\text{m}^2$
c_{fD}	fracture conductivity, dimensionless

h	reservoir thickness, m
μ_g	gas viscosity, mPa·s
B_g	Formation volume factor, m ³ /m ³
φ	reservoir porosity, fraction
t	duration, day
c_g	isothermal gas compressibility factor, 1/MPa
S_{wi}	irreducible water saturation, %
γ_g	specific gravity, fraction
ρ_g	free gas density, kg/m ³
ρ_a	adsorbed gas density, kg/m ³
ρ_b	bulk density of shale, kg/m ³
v_g	Darcy velocity of gas, m/s
V_g	gas volume of adsorption, m ³ /kg
V_L	Langmuir volume, m ³ /kg
Z	gas compressibility factor, fraction
G_p	cumulative gas production, 10 ⁴ m ³
G_{sc}	original gas in place, 10 ⁴ m ³
β	pseudo-time factor, dimensionless
α_t	coefficient, $3.6 \times 24 \times 10^{-3}$
α_p	coefficient, $2\pi \times 3.6 \times 24 \times 10^{-7}$

Special Subscripts:

D	dimensionless
g	gas property
i	initial condition
f	fracture property
sc	standard condition

Appendix A. Derivation of the Model

The analytical solution to the gas flow in a shale gas reservoir can be derived according to the governing equation in porous media:

$$\frac{\partial}{\partial x} \left[\frac{k_g}{\mu_g(p)} \cdot \frac{p}{Z(p)} \frac{\partial p}{\partial x} \right] + \frac{\partial}{\partial y} \left[\frac{k_g}{\mu_g(p)} \cdot \frac{p}{Z(p)} \frac{\partial p}{\partial y} \right] = \frac{1}{\alpha_t} \left[\phi S_g + (1 - \phi) \frac{\partial \rho_a}{\partial \rho_g} \right] \frac{\partial}{\partial t} \left(\frac{p}{Z(p)} \right) \quad (A1)$$

Substituting the pseudo-pressure function into the Equation (A1), the equation that governs the flow in a shale formation is:

$$\frac{\partial^2 p_p(p)}{\partial x^2} = \frac{\phi \mu_{gi} c_{gi} S_g}{\alpha_t k_g} \left[\frac{\mu_g(p) c_g(p)}{\mu_{gi} c_{gi}} + \frac{\mu_g(p) \rho_b}{\mu_{gi} c_{gi} \phi S_g} \frac{p_{sc} Z(p) T}{p Z(p_{sc}) T_{sc}} \frac{V_L p_L}{(p_L + p)^2} \right] \frac{\partial p_p(p)}{\partial t} \quad (A2)$$

Substituting the definition of pseudo-time factor $\beta(t)$ into the Equation (A2), the dimensionless governing equation can be simplified as follows:

$$\frac{\partial^2 p_D}{\partial x_D^2} + \frac{\partial^2 p_D}{\partial y_D^2} = \frac{\partial p_D}{\partial (\beta t_D)} \quad (A3)$$

Definite conditions are:

$$p_D(x_D, y_D, 0) = 0 \quad (A4)$$

$$\frac{\partial p_D(x_{eD}, y_D, \beta t_D)}{\partial x_D} = 0, \frac{\partial p_D(0, y_D, \beta t_D)}{\partial x_D} = 0 \quad (A5)$$

$$\frac{\partial p_D(x_D, y_{eD}, \beta t_D)}{\partial y_D} = 0, \frac{\partial p_D(x_D, 0, \beta t_D)}{\partial y_D} = 0 \quad (A6)$$

As shown in Figure 4, we can obtain that $p_D = p_{ID}$ and $p_D = p_{IID}$ in Region I and Region II respectively. Equation (A3) can be simplified as a group of one-dimensional equations.

(1) In Region I, the linear flow is parallel to the surface of fracture (y -direction), Equation (A3) is simplified as:

$$\frac{\partial^2 p_{ID}}{\partial y_D^2} = \frac{\partial p_{ID}}{\partial (\beta t_{Df})} \quad (\text{A7})$$

Initial condition:

$$p_{ID}(x_D, y_D, 0) = 0 \quad (\text{A8})$$

Boundary condition:

$$\frac{\partial p_{ID}(x_D, y_{eD}, \beta t_{Df})}{\partial y_D} = 0 \quad (\text{A9})$$

Interface conditions:

$$p_{ID}(x_D, \frac{y_{eD}}{2} + y_{fD}, \beta t_{Df}) = p_{IID}(x_D, \frac{y_{eD}}{2} + y_{fD}, \beta t_{Df}) \quad (\text{A10})$$

$$\frac{\partial p_{ID}(x_D, \frac{y_{eD}}{2} + y_{fD}, \beta t_{Df})}{\partial y_D} = \frac{\partial p_{IID}(x_D, \frac{y_{eD}}{2} + y_{fD}, \beta t_{Df})}{\partial y_D} \quad (\text{A11})$$

(2) The flow in the reservoir is mainly the linear flow vertical to the surface of fracture in Region II (dominated in x -direction). The flow in the reservoir can be simplified as follows:

$$\frac{\partial^2 p_{IID}}{\partial x_D^2} + \frac{1}{y_{fD}} \frac{\partial p_{ID}(x_D, \frac{y_{eD}}{2} + y_{fD}, \beta t_{Df})}{\partial y_D} = \frac{\partial p_{IID}}{\partial (\beta t_{Df})} \quad (\text{A12})$$

Initial condition:

$$p_{IID}(x_D, y_D, 0) = 0 \quad (\text{A13})$$

Boundary condition:

$$\frac{\partial p_{IID}(x_{eD}, y_D, \beta t_{Df})}{\partial x_D} = 0 \quad (\text{A14})$$

Interface conditions:

$$p_{IID}(\frac{1}{2}x_{eD} + \frac{1}{2}w_{fD}, y_D, \beta t_{Df}) = p_{fD}(y_D, \beta t_{Df}) \quad (\text{A15})$$

$$\frac{K}{\mu} \frac{\partial p_{IID}(\frac{1}{2}x_{eD} + \frac{1}{2}w_{fD}, y_D, \beta t_{Df})}{\partial x_D} = \frac{K_f}{\mu} \frac{\partial p_{fD}(\frac{1}{2}x_{eD} + \frac{1}{2}w_{fD}, y_D, \beta t_{Df})}{\partial x_D} \quad (\text{A16})$$

(3) It is believed that the steady flow of fluid in the fracture is symmetric (Cinco, 1978). Compared with the entire effective drainage area of the well, the width of the fracture is relatively small. The corresponding dimensionless governing equation is simplified as follows:

$$\frac{d^2 p_{fD}}{dy_D^2} + \frac{2}{c_{fD}} \frac{\partial p_{IID}(\frac{1}{2}x_{eD} + \frac{1}{2}w_{fD}, y_D, \beta t_{Df})}{\partial x_D} = 0 \quad (\text{A17})$$

Outer boundary condition:

$$\frac{dp_{fD}(\frac{1}{2}y_{eD} + y_{fD})}{dy_D} = 0 \quad (\text{A18})$$

Inner boundary condition (constant flow rate or constant bottom-hole pressure):

$$\frac{dp_{fD}(\frac{1}{2}y_{eD})}{dy_D} = -\frac{\pi}{c_{fD}} \quad (\text{A19})$$

$$p_{fD}(\frac{1}{2}y_{eD}) = 1 \quad (\text{A20})$$

The Laplace transform and superposition principle are used to deal with Equations (14)–(17) in Section 3.2 of this article. Then, the pressure distribution function and production behavior of an infinite-conductivity fractured well in the Laplace domain can be derived.

$$s\tilde{p}_{fD}(y_D, s) = \frac{\pi}{c_{fD}} \frac{1}{\sqrt{D(s)}} \frac{\cosh\left(y_D - \frac{1}{2}y_{eD} - y_{fD}\right) \sqrt{D(s)}}{\sinh y_{fD} \sqrt{D(s)}} \quad (\text{A21})$$

$$s\tilde{q}_{wD}(y_D, s) = \frac{c_{fD}}{\pi} \sqrt{D(s)} \cdot \frac{\sinh y_{fD} \sqrt{D(s)}}{\cosh\left(y_D - \frac{1}{2}y_{eD} - y_{fD}\right) \sqrt{D(s)}} \quad (\text{A22})$$

where:

$$D(s) = 2C(s)/c_{fD}; C(s) = \sqrt{B(s)} \tanh(x_{eD} - \frac{1}{2}x_{eD} - \frac{1}{2}w_{fD}) \sqrt{B(s)};$$

$$B(s) = s + \frac{1}{y_{fD}} A(s); A(s) = \sqrt{s} \tanh(y_{eD} - \frac{1}{2}y_{eD} - y_{fD}) \sqrt{s}.$$

References

1. Jarvie, D.M. Shale resource systems for oil and gas: Part 1—Shale-gas resource systems. *AAPG Mem.* **2012**, *97*, 69–87.
2. Zhang, L.; Pan, R. Major Accumulation Factors and Storage Reconstruction of Shale Gas Reservoir. *China Pet. Explor.* **2009**, *14*, 20–23.
3. Hu, Z.; Du, W.; Peng, Y.; Zhao, J. Microscopic pore characteristics and the source-reservoir relationship of shale—A case study from the Wufeng and Longmaxi Formations in Southeast Sichuan Basin. *Oil Gas Geol.* **2015**, *36*, 1001–1008.
4. Martin, J.P.; Hill, D.G.; Lombardi, T.E.; Nyahay, R. A Primer on New York's Gas Shales. In *Field Trip Guidebook for the 80th Annual Meeting of the New York State Geological Association*; New York State Geological Association: New York, NY, USA, 2010; pp. A1–A32.
5. Tinni, A.; Sondergeld, C.; Rai, C. New Perspectives on the Effects of Gas Adsorption on Storage and Production of Natural Gas from Shale Formations. In Proceedings of the SPWLA 58th Annual Logging Symposium, Oklahoma, OK, USA, 17–21 June 2017; Society of Petrophysicists and Well-Log Analysts: Houston, TX, USA, 2017.
6. Zhang, K.; Wang, M.; Liu, Q.; Wu, K.; Yu, L.; Zhang, J.; Chen, S. Effects of Adsorption and Confinement on Shale Gas Production Behavior. In Proceedings of the SPE/IATMI Asia Pacific Oil & Gas Conference and Exhibition, Bali, Indonesia, 20–22 October 2015; Society of Petroleum Engineers: Richardson, TX, USA, 2015.
7. Mengal, S.A.; Wattenbarger, R.A. Accounting for adsorbed gas in shale gas reservoirs. In Proceedings of the SPE Middle East Oil and Gas Show and Conference, Manama, Bahrain, 25–28 September 2011; SPE 141085; Society of Petroleum Engineers: Richardson, TX, USA, 2011; pp. 1–15.
8. Thompson, J.M.; M'Angha, V.O.; Anderson, D.M. Advancements in shale gas production forecasting—a Marcellus case study. In Proceedings of the SPE Americas Unconventional Gas Conference and Exhibition, The Woodlands, TX, USA, 14–16 June 2011; SPE 144436; Society of Petroleum Engineers: Richardson, TX, USA, 2011.
9. Arps, J.J. Analysis of decline curves. *Trans. AIME* **1945**, *160*, 228–247. [[CrossRef](#)]
10. Solar, C.; Blanco, A.G.; Vallone, A.; Sapag, K. Adsorption of Methane in porous materials as the basis for the storage of natural gas. In *Natural Gas*; InTech: Rijeka, Croatia, 2010.
11. Busch, A.; Alles, S.; Gensterblum, Y.; Prinz, D.; Dewhurst, D.N.; Raven, M.D.; Stanjek, H.; Krooss, B.M. Carbon dioxide storage potential of shales. *Int. J. Greenh. Gas Control* **2008**, *2*, 297–308. [[CrossRef](#)]
12. Guo, W.; Xiong, W.; Gao, S.; Hu, Z. Isothermal adsorption/desorption characteristics of shale gas. *J. Cent. South Univ.* **2013**, *44*, 2836–2840.
13. Clarkson, C.; Haghshenas, B. Modeling of Supercritical Fluid Adsorption on Organic-Rich Shales and Coal. In Proceedings of the SPE Unconventional Resources Conference-USA, The Woodlands, TX, USA, 10–12 April 2013; SPE 164532. Society of Petroleum Engineers: Richardson, TX, USA, 2013; pp. 1–24.
14. Cipolla, C.L.; Lolon, E.P.; Erdle, J.C.; Rubin, B. Reservoir modeling in shale-gas reservoirs. *SPE Res. Eval. Eng.* **2010**, *13*, 638–653. [[CrossRef](#)]

15. Das, M.; Jonk, R.; Schelble, R. Effect of multicomponent adsorption/desorption behavior on Gas-In-Place (GIP) calculations and estimation of free and adsorbed CH₄ and CO₂ in shale gas systems. In Proceedings of the Annual Technical Conference and Exhibition, San Antonio, TX, USA, 8–10 October 2012; SPE 159558; Society of Petroleum Engineers: Richardson, TX, USA, 2012.
16. Coletti, K. Hydraulic Fracturing in the Marcellus Shale Region of the US. 1970. Available online: <http://www.northeastern.edu/nuwwriting/hydraulic-fracturing-in-the-marcellus-shale-region-of-the-u-s/> (accessed on 11 October 2017).
17. Frohne, K.H.; Mercer, J.C. Fractured Shale Gas Reservoir Performance Study-An Offset Well Interference Field Test. *J. Pet. Technol.* **1984**, *36*, 291–300. [[CrossRef](#)]
18. Chen, C.; Ozkan, E.; Raghavan, R. A Study of Fractured Wells in Bounded Reservoirs. In Proceedings of the SPE Annual Technical Conference and Exhibition, Dallas, TX, USA, 6–9 October 1991; SPE 22717; Society of Petroleum Engineers: Richardson, TX, USA, 1991; pp. 565–576.
19. Zhang, X.; Du, C.; Deimbacher, F.; Crick, M.; Harikesavanallur, A. Sensitivity Studies of Horizontal Wells with Hydraulic Fractures in Shale Gas Reservoirs. In Proceedings of the International Petroleum Technology Conference, Doha, Qatar, 7–9 December 2009; pp. 1–9, IPTC 13338.
20. Deng, J.; Zhu, W.; Ma, Q. A new seepage model for shale gas reservoir and productivity analysis of fractured well. *Fuel* **2014**, *124*, 232–240. [[CrossRef](#)]
21. Zhang, D.; Zhang, L.; Guo, J.; Zhou, Y.; Zhao, Y. Research on the production performance of multistage fractured horizontal well in shale gas reservoir. *J. Nat. Gas Sci. Eng.* **2015**, *26*, 279–289. [[CrossRef](#)]
22. Wanniarachchi, W.A.M.; Ranjith, P.G.; Perera, M.S.A.; Lashin, A.; Al Arifi, N.; Li, J.C. Current opinions on foam-based hydro-fracturing in deep geological reservoirs. *Geomech. Geophys. Geo-Energy Geo-Resour.* **2015**, *1*, 121–134. [[CrossRef](#)]
23. Ma, T.; Chen, P.; Zhao, J. Overview on vertical and directional drilling technologies for the exploration and exploitation of deep petroleum resources. *Geomech. Geophys. Geo-Energy Geo-Resour.* **2016**, *2*, 365–395. [[CrossRef](#)]
24. Wang, W.; Zheng, D.; Sheng, G.; Zhang, Q.; Su, Y. A review of stimulated reservoir volume characterization for multiple fractures horizontal well in unconventional reservoirs. *Adv. Geo-Energy Res.* **2017**, *1*, 54–63.
25. Wattenbarger, R.A.; El-Banbi, A.H.; Vilegas, M.E.; Maggard, J.B. Production analysis of linear flow into fractured tight gas wells. In Proceedings of the SPE Rocky Mountain Regional/Low-Permeability Reservoirs Symposium, Denver, CO, USA, 5–8 April 1998; SPE 39931; Society of Petroleum Engineers: Richardson, TX, USA, 1998; pp. 1–12.
26. Cinco, L.; Samaniego, V.; Dominguez, A. Transient pressure behavior for a well with a finite-conductivity vertical fracture. *Soc. Pet. Eng. J.* **1978**, *18*, 253–264. [[CrossRef](#)]
27. Cinco, L.; Satnaniago, V. Transient pressure analysis for fractured wells. *J. Pet. Technol.* **1981**, *33*, 1749–1766. [[CrossRef](#)]
28. Brown, M.; Ozkan, E.; Raghavan, R.; Kazemi, H. Practical solutions for pressure transient responses of fractured horizontal wells in unconventional reservoirs. *SPE Reserv. Eval. Eng.* **2009**, *14*, 663–676. [[CrossRef](#)]
29. Lee, S.; Brockenbrough, J. A new approximate analytic solution for finite-conductivity vertical fractures. *SPE Form. Eval.* **1986**, *1*, 75–88. [[CrossRef](#)]
30. Azari, M.; Wooden, W.; Coble, L. A complete set of Laplace transforms for finite-conductivity vertical fractures under bilinear and trilinear flows. In Proceedings of the SPE Annual Technical Conference and Exhibition, New Orleans, LA, USA, 23–26 September 1990; SPE 20556. Society of Petroleum Engineers: Richardson, TX, USA, 1990; pp. 251–266.
31. Azari, M.; Wooden, W.; Coble, L. *Further Investigation on the Analytic Solution for Finite-Conductivity Vertical Fractures*; SPE 21402; Society of Petroleum Engineers: Richardson, TX, USA, 1991; pp. 559–576.
32. Meyer, B.R.; Bazan, L.W.; Jacot, R.H.; Lattibeaudiere, M.G. *Optimization of Multiple Transverse Hydraulic Fractures in Horizontal Wellbores*; SPE 131733; Society of Petroleum Engineers: Richardson, TX, USA, 2010; pp. 1–37.
33. Brohi, I.; Pooladi-Darvish, M.; Aguilera, R. *Modeling Fractured Horizontal Wells as Dual Porosity Composite Reservoirs-Application to Tight Gas, Shale Gas and Tight Oil Cases*; SPE 144057; Society of Petroleum Engineers: Richardson, TX, USA, 2011; pp. 1–22.
34. Stalgorova, E.; Mattar, L. *Analytical Model for History Matching and Forecasting Production in Multifrac Composite Systems*; SPE 162516; Society of Petroleum Engineers: Richardson, TX, USA, 2012; pp. 1–17.

35. Stalgorova, E.; Mattar, L. *Practical Analytical Model to Simulate Production of Horizontal Wells with Branch Fractures*; SPE 162515; Society of Petroleum Engineers: Richardson, TX, USA, 2012; pp. 1–17.
36. Yao, S.; Wang, X.; Zeng, F.; Li, M.; Ju, N. *A Composite Model for Multi-Stage Fractured Horizontal Wells in Heterogeneous Reservoirs*; SPE 182016; Society of Petroleum Engineers: Richardson, TX, USA, 2016; pp. 1–32.
37. Guo, J.; Zeng, J.; Wang, X.; Zeng, F. *Analytical Model for Multifractured Horizontal Wells in Heterogeneous Shale Reservoirs*; SPE 182422; Society of Petroleum Engineers: Richardson, TX, USA, 2016; pp. 1–41.
38. Zhang, M.; Vardcharragosad, P.; Ayala, H. The similarity theory applied to early-transient gas flow analysis in unconventional reservoirs. *J. Nat. Gas Sci. Eng.* **2014**, *21*, 659–668. [[CrossRef](#)]
39. Nobakht, M.; Clarkson, C. *A New Analytical Method for Analyzing Linear Flow in Tight/Shale Gas Reservoirs: Constant-Flowing-Pressure Boundary Condition*; SPE 143989; Society of Petroleum Engineers: Richardson, TX, USA, 2012; pp. 370–384.
40. Qanbari, F.; Clarkson, C. A new method for production data analysis of tight and shale gas reservoirs during transient linear flow period. *J. Nat. Gas Sci. Eng.* **2013**, *14*, 55–65. [[CrossRef](#)]
41. Liu, H.H.; Ranjith, P.G.; Georgi, D.T.; Lai, B.T. Some key technical issues in modelling of gas transport process in shales: A review. *Geomech. Geophys. Geo-Energy Geo-Resour.* **2016**, *2*, 231–243. [[CrossRef](#)]
42. Lee, W.J.; Holditch, S.A. Application of pseudotime to buildup test analysis of low-permeability gas wells with long-duration wellbore storage distortion. *J. Pet. Technol.* **1982**, *34*, 2877–2887. [[CrossRef](#)]
43. Blasingame, T.A.; Lee, W.J. The variable-rate reservoir limits testing of gas wells. In Proceedings of the SPE Gas Technology Symposium, Dallas, TX, USA, 13–15 June 1988; Society of Petroleum Engineers: Richardson, TX, USA, 1988.
44. Stanislav, J.F.; Kabir, C.S. *Pressure Transient Analysis*; Prentice Hall: Englewood Cliffs, NJ, USA, 1990.
45. Raghavan, R. *Well Test Analysis*; Prentice Hall: Englewood Cliffs, NJ, USA, 1993.
46. Palacio, J.C.; Blasingame, T.A. *Decline Curve Analysis Using Type Curves—Analysis of Gas Well Production Data*; SPE 25909; Society of Petroleum Engineers: Richardson, TX, USA, 1993; pp. 12–14.
47. Horne, R.N. *Modern Well Test Analysis: A Computer-Aided Approach*; Petroway: Palo Alto, CA, USA, 1995.
48. Lee, J.; Rollins, J.B.; Spivey, J.P. *Pressure Transient Testing*; SPE Textbook Series vol. 9; Society of Petroleum Engineers: Richardson, TX, USA, 2003.
49. Kamal, M.M. *Transient Well Testing*; Monograph Series Vol. 23; Society of Petroleum Engineers: Richardson, TX, USA, 2009.
50. Sing, K.S.W.; Everett, D.H.; Haul, R.A.W.; Moscou, L.; Pierotti, R.A.; Rouquerol, J.; Siemieniewska, T. Reporting Physisorption Data for Gas/Solid Systems with Special Reference to the Determination of Surface Area and Porosity (Recommendations 1984). *Pure Appl. Chem.* **1985**, *57*, 603–619. [[CrossRef](#)]
51. Sheindorf, C.H.; Rebhun, M.; Sheintuch, M. A Freundlich-type multicomponent isotherm. *J. Colloid Interface Sci.* **1981**, *79*, 136–142. [[CrossRef](#)]
52. Dubinin, M.M. Fundamentals of the theory of adsorption in micropores of carbon adsorbents: Characteristics of their adsorption properties and microporous structures. *Carbon* **1989**, *27*, 457–467. [[CrossRef](#)]
53. Langmuir, I. The Adsorption of Gases on Plane Surfaces of Glass, Mica and Platinum. *J. Am. Chem. Soc.* **1918**, *40*, 1403–1461. [[CrossRef](#)]
54. Patzek, T.; Male, F.; Marder, M. Gas Production in the Barnett Shale Obeys a Simple Scaling Theory. *Proc. Natl. Acad. Sci. USA* **2013**, *110*, 19731–19736. [[CrossRef](#)] [[PubMed](#)]
55. Yu, W.; Sepehrnoori, K. Simulation of Gas Desorption and Geomechanics Effects for Unconventional Gas Reservoirs. *Fuel* **2014**, *116*, 455–464. [[CrossRef](#)]
56. Russell, D.G.; Goodrich, J.H.; Perry, G.E.; Bruskotter, J.F. *Methods of Predicting Gas Well Performance*; Paper SPE; Society of Petroleum Engineers: Richardson, TX, USA, 1966; pp. 99–108.
57. Ye, P.; Ayala, H.L.F. A density-diffusivity approach for the unsteady state analysis of natural gas reservoirs. *J. Nat. Gas Sci. Eng.* **2012**, *7*, 22–34. [[CrossRef](#)]
58. Fraim, M.; Wattenbarger, R. Gas reservoir decline curve analysis using type curves with real gas pseudopressure and normalized time. *SPE Form. Eval.* **1987**, *2*, 671–682. [[CrossRef](#)]
59. King, G.R. *Material Balance Techniques for Coal Seam and Devonian Shale Gas Reservoirs*; SPE 20730; Society of Petroleum Engineers: Richardson, TX, USA, 1990; pp. 182–192.
60. Moghadam, S.; Jeje, O.; Mattar, L. Advanced gas material balance in simplified format. *J. Can. Pet. Technol.* **2009**, *50*, 90–98. [[CrossRef](#)]
61. Stehfest, H. Numerical Inversion of Laplace Transforms. *Commun. ACM* **1970**, *13*, 47–49. [[CrossRef](#)]

62. Van Everdingen, A.F.; Hurst, W. *The Application of The Laplace Transformation to Flow Problems in Reservoirs*; Society of Petroleum Engineers: Richardson, TX, USA, 1949.
63. Molina, O.; Zeidouni, M. An Enhanced Nonlinear Analytical Model for Unconventional Multifractured Systems. In Proceedings of the SPE Europec Featured at 79th EAGE Conference and Exhibition, Paris, France, 12–15 June 2017; Society of Petroleum Engineers: Richardson, TX, USA, 2017.
64. IHS Harmony. Analysis Method Theory, IHS Inc. 2016. Available online: <https://www.ihs.com/btp/fekete.html> (accessed on 11 October 2017).
65. IHS Course Manual Software Training Course: IHS Harmony and IHS Decline Plus Training. 2017. Available online: <https://www.ihs.com/products/declineplus-training.html> (accessed on 11 October 2017).



© 2017 by the authors. Licensee MDPI, Basel, Switzerland. This article is an open access article distributed under the terms and conditions of the Creative Commons Attribution (CC BY) license (<http://creativecommons.org/licenses/by/4.0/>).